

**Sea salt aerosols as a reactive surface for inorganic and
organic acidic gases in the arctic troposphere**

**J. W. Chi¹, W. J. Li^{1,*}, D. Z. Zhang², J. C. Zhang³, Y. T. Lin³, X. J. Shen⁴, J. Y.
Sun⁴, J. M. Chen¹, X. Y. Zhang⁴, Y. M. Zhang^{4,*}, W. X. Wang¹**

[1] Environment Research Institute, Shandong University, Jinan, Shandong 250100,
China

[2] Faculty of Environmental and Symbiotic Sciences, Prefectural University of
Kumamoto, Kumamoto 862-8502, Japan

[3] Key Laboratory of the Earth' Deep Interior, Institute of Geology and Geophysics,
Chinese Academy of Sciences, Beijing 100029, China

[4] Key Laboratory of Atmospheric Chemistry of CMA, Institute of Atmospheric
Composition, Chinese Academy of Meteorological Sciences, Beijing 100081, China

*Correspondence to: W. J. Li (liweijun@sdu.edu.cn)

Y. M. Zhang (ymzhang@cams.cma.gov.cn)

Abstract

Sea salt aerosols (SSA) are dominant particles in the arctic atmosphere and determine the polar radiative balance. SSA react with acidic pollutants that lead to changes of physical and chemical properties of their surface, which in turn alter their hygroscopic and optical properties. Transmission electron microscopy with energy-dispersive X-ray spectrometry was used to analyze morphology, composition, size, and mixing state of individual SSA at Ny-Ålesund, Svalbard in summertime. Individual fresh SSA contained cubic NaCl coated by certain amounts of MgCl₂ and CaSO₄. Individual partially aged SSA contained irregular NaCl coated by a mixture of NaNO₃, Na₂SO₄, Mg(NO₃)₂, and MgSO₄. The comparison suggests the hydrophilic MgCl₂ coating in fresh SSA likely intrigued the heterogeneous reactions at the beginning of SSA and acidic gases. Individual fully aged SSA normally had Na₂SO₄ cores and an amorphous coating of NaNO₃. Elemental mappings of individual SSA particles revealed that as the particles ageing Cl gradually decreased but the C, N, O, and S content increased. ¹²C⁻ mapping from nanoscale secondary ion mass spectrometry indicates that organic matter increased in the aged SSA compared with the fresh SSA. ¹²C⁻ line scan further shows that organic matter was mainly concentrated on the aged SSA surface. These new findings indicate that this mixture of organic matter and NaNO₃ on particle surfaces likely determines their hygroscopic and optical properties. These abundant SSA as reactive surfaces absorbing inorganic and organic acidic gases can shorten acidic gas lifetime and influence the possible gaseous reactions in the arctic atmosphere, which need to be incorporated into atmospheric chemical models in the arctic troposphere.

1 **1 Introduction**

2 The arctic atmosphere was long believed to be an extremely clean background
3 laboratory to research aerosol chemical processes, transport of atmospheric aerosols,
4 and their impact on global climate (Law and Stohl, 2007). In the last decades,
5 however, arctic temperatures have increased at twice the global average rate (Serreze
6 and Francis, 2006), resulting in a dramatic decrease of Arctic pack ice (Lindsay et al.,
7 2009). This arctic climate change has been attributed to the increase of greenhouse
8 gases in the troposphere (Vavrus, 2004) and to anthropogenic emissions of air
9 pollutants from the middle latitudes (Barrie, 1986;Iziomon et al., 2006;Law and Stohl,
10 2007). In particular, the “Arctic Haze” phenomenon caused by the long-range
11 transport of anthropogenic emissions (e.g., organic acids, H₂SO₄/SO₂, and HNO₃/NO_x)
12 from lower latitudes has received increasing attention in the last thirty years
13 (Heintzenberg, 1980;Shaw, 1995;Law and Stohl, 2007).

14 Various aerosol particles from industrial, urban, and marine emissions occur in
15 the arctic atmosphere (Goto-Azuma and Koerner, 2001;Ghorai et al., 2014). Black
16 carbon as one solar absorber in the troposphere and in the snow or ice (Hegg et al.,
17 2009) can amplify the change of the arctic climate (Sand et al., 2013). In addition,
18 H₂SO₄/SO₂ and HNO₃/NO_x from anthropogenic sources in middle latitudes are
19 transported into the central arctic area (Law and Stohl, 2007), where they react with
20 sea salt aerosols (SSA) (Hara et al., 2003;Geng et al., 2010;Sierau et al., 2014). SSA
21 have reactive surfaces that can easily participate in heterogeneous and multiphase
22 chemical reactions (Rossi, 2003) and play a significant role in the global S and N
23 cycle (Pósfai et al., 1994;Sierau et al., 2014). These aged SSA not only affect
24 incoming solar radiation by scattering or absorbing directly (Murphy et al., 1998), but
25 also can serve as cloud condensation nuclei (CCN) or ice nuclei (IN) and further alter
26 cloud properties (Hu et al., 2005;Leck and Svensson, 2015). It was also proved that
27 such cloud changes cause 40% of the arctic warming (Vavrus, 2004). Understanding
28 the chemical composition of the arctic SSA is critical to understand how they affect
29 the polar climate (Hara et al., 2003).

30 SSA have been intensively studied in both laboratory and field experiments in

1 coastal areas (O'Dowd et al., 1997; O'Dowd and De Leeuw, 2007; Yao and Zhang,
2 2011; Li et al., 2011b; Laskin et al., 2012; Ault et al., 2012; Ghorai et al., 2014). In
3 laboratory studies Ault et al. (2013a) suggested spatial redistribution of the cations
4 (Na^+ , K^+ , Mg^{2+} , and Ca^{2+}) between core and surface after heterogeneous reaction of
5 SSA and nitric acids. Deliquescence-mode experiments with mixed $\text{NaCl}/\text{MgSO}_4$
6 aerosol particles show that Mg salts (e.g., MgSO_4 and MgCl_2) concentrated in the
7 surface can easily take up water and lower the deliquescence point of NaCl particles
8 (Woods et al., 2010). Hara et al. (2003) suggested that most SSA play a pivotal role in
9 the lower troposphere (< 3 km) and result in noticeable depletion of chlorine in the
10 arctic. Laskin et al. (2012) found that SSA may effectively react with organic acids,
11 leaving behind particles depleted in chloride and enriched in the corresponding
12 organic salts in one polluted coastal area. Organic acids can react with SSA and
13 change their hygroscopicity in polluted continental air (Ghorai et al., 2014), which can
14 alter their heterogeneous reactions and CCN activity (Laskin et al., 2012). In light of
15 the limited microscopic observations of arctic aerosols, at least two questions have not
16 been answered. Firstly, detailed information about ageing processes of SSA surfaces
17 has not been determined in the arctic atmosphere. Secondly, to what degree do organic
18 acids react with SSA in the clean atmosphere? This knowledge is critical to
19 understand how small amounts of anthropogenic gases (e.g., organic acids,
20 $\text{H}_2\text{SO}_4/\text{SO}_2$, and HNO_3/NO_x) affect the hygroscopic and optical properties of SSA in
21 the clean arctic atmosphere.

22 To characterize individual SSA collected on August 3-23, 2012, at the Chinese
23 Arctic Yellow River Station, we applied different microscopic techniques with
24 resolution down to the nanometer scale: transmission electron microscopy with
25 energy-dispersive X-ray spectrometry (TEM/EDX), scanning electron microscopy
26 (SEM), scanning TEM (STEM), and atomic force microscopy (AFM), and nanoscale
27 secondary ion mass spectrometry (nanoSIMS). The different types of individual SSA
28 were identified based on their morphology and composition. Elemental and ion
29 mappings revealed mixing properties of different species in individual SSA which
30 further participated in chemical reactions in the clean Arctic atmosphere. The dual

aims of our study are to explain the need to understand the complexity of realistic atmospheric SSA and to provide fundamental experimental data to understand heterogeneous reactions of SSA in the clean arctic atmosphere.

2 Experiments

2.1 Sampling

Svalbard is an archipelago in the Arctic Ocean consisting of Spitsbergen, Bear Island, and Hopen, which together cover about 62,000 km². Ny-Ålesund, whose geographical coordinates are 78°55'N, 11°56'E, is situated on the west coast of Spitsbergen and is an international center of scientific research and environmental monitoring in the central Arctic.

Aerosol samples were collected from 3 to 23 August, 2012, using an individual particle sampler at the Chinese Arctic Yellow River Station, Ny-Ålesund (Fig. S1). We use copper TEM grids coated with carbon film (carbon type-B, 300-mesh copper, Tianld Co., China) to collect aerosols by a single-stage cascade impactor with a 0.5-mm-diameter jet nozzle at a flow rate of 1.0 L min⁻¹. The collection efficiency of the impactor is 50% for particles with an aerodynamic diameter of 0.3 μm and almost 100% at 0.5 μm if the density of particles is 2 g cm⁻³. The sampling duration of each sample varied from twenty minutes to two hours depending on the aerosol dispersion on the film that was estimated by optical microscopy after the sampling. Then we placed the grids in sealed, dry, plastic capsules to prevent contamination. Finally, the samples were stored in a desiccator at 25 °C and 20±3% relative humidity (RH) until analysis (Li et al., 2011a).

According to the sampling time and sample quality, 23 aerosol samples were selected for analysis with TEM. During the sampling periods, temperatures were 1.6~7.3 °C; RH, 56~94%; air pressure, 997.0~1020.7 hPa; and sampling wind speeds, 0~8.9 m s⁻¹. Detailed sampling information can be found in Table S1.

2.2 Electron microscopic analyses

Individual particle samples were examined by a JEOL JEM-2100 transmission electron microscopy operated at 200 kV with energy-dispersive X-ray spectrometry

(TEM/EDX) and scanning electron microscopy (SEM; Philips XL30) operated at a 20 kV accelerating voltage and a 80 μ A filament. EDX spectra were examined within a maximum time of 30 s to minimize potential beam damage and efficiently collect particle elemental composition. TEM grids were made of copper (Cu) and covered by a carbon-reinforced substrate, so Cu had to be excluded from the quantitative analyses of the particles while residual C content was detected and overestimated in EDX spectra of individual particles. Elemental composition, morphology, size distribution, and mixing state have been studied by the TEM/EDX. Both submicron and supermicron particles occur on the TEM grids: coarser particles occur near the center, and finer particles are on the periphery (Li and Shao, 2009). To be more representative, 4-5 areas from the center to periphery of the sampling spot were chosen to analyze all the particles. Altogether we analyzed 1577 aerosol particles to understand the details of their mixing states, both internal and external. We used iTEM software to analyze the TEM images and obtained area, circularity, perimeter, and equivalent circle diameter of individual aerosol particles.

Some typical aerosol particles were analyzed for elemental mapping with a JEOL JEM-2100F TEM with scanning TEM (STEM) operation mode. Elemental mappings were collected in the annular dark-field imaging mode, with the electron beam focused on a corresponding spot of the sample but then scanned over this area in a raster. Elemental mapping has become an important tool in individual particle analysis in the recent years (Ault et al., 2012; Li et al., 2013a; Li et al., 2013b), because it clearly displays the distribution of the detectable elements within each particle.

2.3 NanoSIMS analysis

Individual aerosol particles were analyzed using a nanoscale secondary ion mass spectrometer (nanoSIMS) 50L (CAMECA Instruments, Geneviers, France), an ultra-high vacuum technique for surface and thin-film analysis at the Institute of Geology and Geophysics, Chinese Academy of Sciences. In this study, $^{12}\text{C}^-$, $^{16}\text{O}^-$, $^{12}\text{C}^{14}\text{N}^-$, $^{14}\text{N}^{16}\text{O}_2^-$, $^{32}\text{S}^-$, $^{35}\text{Cl}^-$, and $^{23}\text{Na}^{16}\text{O}^-$ ions in individual particles were obtained when the Cs^+ primary ion beam caused the ionization of atoms within the particles. Furthermore, ion intensity mappings of individual particles with nanometer resolution

can show the distribution of different ions. $^{12}\text{C}^-$ represents the organic matter in individual particles that excludes the contribution from the carbon substrate. Laboratory generated NaNO_3 particles on silicon substrate analyzed by nanoSIMS show $^{14}\text{N}^{16}\text{O}_2^-$ and $^{23}\text{Na}^{16}\text{O}^-$ are their markers (Fig. S3).

2.4 AFM analysis

Atomic force microscopy (AFM) with a tapping mode analyzed aerosol particles under ambient conditions. AFM, a digital NanoscopeIIIa Instrument, can detect the three-dimensional morphology of particles. The AFM settings contain imaging forces between 1 and 1.5 nN, scanning rates between 0.5 and 0.8 Hz, and scanning range sizes at 10 μm with a resolution of 512 pixels per length. After the AFM analysis, composition of the same particles was confirmed by TEM, with twelve SSA particles analyzed by this method. The NanoScope analysis software can automatically obtain bearing area (A) and bearing volume (V) of each analyzed particle according to the following formula.

$$A = \frac{4}{3}\pi r^2 = \frac{\pi d^2}{3} \rightarrow d = \sqrt{\frac{3A}{\pi}} \quad (1)$$

$$V = \frac{4}{3}\pi r^3 = \frac{4}{3}\pi \times \frac{D^3}{8} \rightarrow D = \sqrt[3]{\frac{6V}{\pi}} \quad (2)$$

Where d is the equivalent circle diameter and D the equivalent volume diameter.

Additionally, we know the relation between d and D is $D = 0.7487 \times d$, as shown in Fig. S2. As a result, equivalent circle diameter (d) of individual aerosol particles measured from the iTEM software can be further converted into equivalent volume diameter (D) based on this relationship.

3 Results

3.1 Types and size distribution of Arctic aerosol particles

Based on their different morphology and composition, aerosol particles were divided into four major categories: sea salt (Fig. 1A-a), S-rich (OC-coating) (Fig. 1A-b), Ca/Mg-S/N/Cl (Fig. 1A-c) and mineral (Fig. 1A-d). TEM observations indicated that SSA were most abundant from 100 nm to 10 μm in the summer arctic

atmosphere. Figure 1B shows that the relative abundance of SSA in the samples was about 72% of the total aerosols. This result is consistent with the dominant SSA in different seasons reported for the arctic atmosphere (Hara et al., 2003;Geng et al., 2010).

3.2 The microscopic characterization and elements of SSA

Based on their morphology and composition, we can further identify three types of SSA: fresh SSA, partially aged SSA, and fully aged SSA.

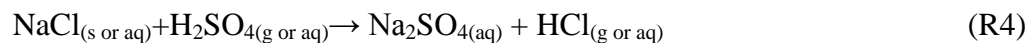
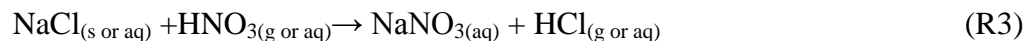
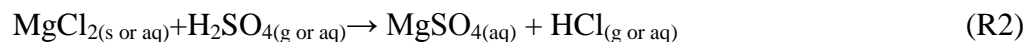
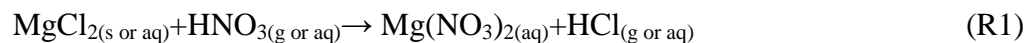
3.2.1 Fresh SSA

The fresh SSA refer to particles which have not experienced any atmospheric chemical modification after emission. TEM and SEM images clearly show that individual fresh SSA include the cubic NaCl core with MgCl₂ and CaSO₄ coating (Fig. 2). Figure 2i shows that the NaCl core only contains Na and Cl with their ionic concentration ratio (Na/Cl) close to 1:1. The coating contains appropriate quantities of Mg, Ca, S, O and Cl, which could be defined as CaSO₄, MgCl₂, and other species (Figs. 2j, k, l). NaCl particles surrounded by the Mg-rich and Ca-rich coatings have been inferred by SEM and TEM (Pósfai et al., 1994;Murphy et al., 1998;Hara et al., 2003;Geng et al., 2010), but the details about the coatings have not been revealed in the Arctic atmosphere. In this study, the high-resolution TEM and SEM images displayed the accurate mixing structures of NaCl and other species. Here we identified two kinds of fresh SSA: one, a NaCl core encased by a distinct coating of CaSO₄ and Mg-rich (MgCl₂) materials (e.g., Figs. 2a-d); and another, a NaCl core encased by a mixture of Mg-rich and Ca-rich materials (e.g., Figs. 2e-f).

3.2.2 Partially aged SSA

Partially aged SSA, we define as those particles that experience atmospheric chemical modifications on their surfaces but retain the NaCl core. Figures 3a-f show that individual partially aged SSA clearly include NaCl core and coating. The morphology of the partially aged SSA differ from the fresh ones as shown in the TEM images of Figs. 2 and 3. Figure 3 shows that the core still keeps the crystalline phase of NaCl with its irregular shape and that the coatings mainly consist of Na, Mg, Ca, K, O, and S with either negligible or minor Cl. Typical Cl-depletion phenomena suggest

that the SSA likely underwent chemical ageing in the atmosphere, as below:



(s, solid; aq, aqueous; and g, gaseous)

Similar chemical reactions on SSA have been detected in both coastal air and laboratory experiments (Allen et al., 1996; Gard et al., 1998; Kouyoumdjian and Saliba, 2006; Ault et al., 2013a). These heterogeneous chemical reactions significantly change the morphology and composition of SSA. Our results suggest that the MgCl_2 coatings in fresh SSA were converted into a more complex coating mixture of MgSO_4 , $\text{Mg}(\text{NO}_3)_2$, Na_2SO_4 , and NaNO_3 in partially aged SSA.

3.2.3 Fully aged SSA

In fully aged SSA the NaCl core has been completely transformed into NaNO_3 and Na_2SO_4 through atmospheric heterogeneous chemical reactions with acidic gases. Figure 4 shows that the fully aged SSA have completely lost their NaCl core, suggesting that the Cl in SSA was completely depleted through heterogeneous chemical reactions, such as reactions (R1)-(R4). The rod-like Na_2SO_4 aggregates comprising the core were frequently internally mixed with NaNO_3 . TEM study indicates that Na_2SO_4 and NaNO_3 are crystalline and amorphous materials, respectively. The fully aged SSA (Fig. 4) on the substrate become more round compared with fresh SSA (Fig. 2) and partially aged SSA (Fig. 3).

3.3 The SSA ageing and back trajectories of air masses

To summarize three types of SSA, we make one Na-Cl-O triangular diagram. Figure 5 gives general information about Cl depletion among the fresh, partially aged, and fully aged SSA. Three particle types in the triangular diagram display interesting distribution: the fresh SSA around the NaCl , the partially aged SSA in the center of triangular (including partial NaCl), the fully aged SSA around NaNO_3 , and Na_2SO_4 (chloride full depletion).

Three-day (72h) back trajectories of air masses were generated using the HYSPLIT model at the Chinese Arctic Yellow River Station during August 3-23, 2012, at an altitude of 500 m above the sea level (Fig. 6). Most air masses originate in the Arctic Ocean, and are restricted to this vast marine region during the sampling periods. Figure 6 shows that two groups of back trajectories exhibit different ageing degree of SSA: One group originates from central Arctic Ocean and other one from North America and Greenland. Fractions of the fresh, partially aged, and fully aged SSA are 43.07%, 44.53%, and 12.41% in first group and 18.72%, 47.45%, 33.83% in second group, respectively (Fig. 6). As a result, air masses from North America and Greenland brought large amounts of aged SSA into the arctic area in summertime.

3.4 Size distribution of individual SSA

Figure 7 shows size distributions of the fresh, partially aged, and fully aged SSA. The peaks of fresh and partially aged SSA are 0.68 μm and 1.30 μm , respectively, and the fully aged ones display a broad size range from 0.9 μm to 2.0 μm (Fig. 7). Our results show that the average particle sizes gradually increase from fresh SSA, partially aged SSA, to fully aged SSA. Therefore, dry and wet deposition of aerosol particles could be changed following the degree of the particles ageing.

4 Discussion

4.1 Sulfate and nitrate formation in individual SSA

TEM observations classified the SSA into fresh, partially aged, and fully aged SSA in the arctic atmosphere. Using individual particle analysis of the three types of SSA, it is shown that there is a major change of their internal structure and composition. The STEM further determined elemental mappings of Na, Mg, Ca, Cl, S, O, C, and N in the three kinds of SSA. Elemental mapping can clearly display the elemental distribution within each particle, which indicates the possible heterogeneous chemical reactions on their surfaces (Conny and Norris, 2011; Ault et al., 2012). Figure 8 shows that Cl content decreases and S, O, C and N contents increase from partially aged (particle B) to fully aged SSA (particle C). Na-Cl-O triangular diagram further shows that Cl in SSA has been depleted and O content increases likely through additional chemical reactions (Fig. 5). Figure 9a shows $^{35}\text{Cl}^-$ in the NaCl core and minor $^{16}\text{O}^-$ and $^{32}\text{S}^-$ in the coating in fresh SSA. Figure 9b shows

the absence of $^{35}\text{Cl}^-$ and the high intensity of $^{16}\text{O}^-$, $^{14}\text{N}^{16}\text{O}_2^-$, $^{32}\text{S}^-$, and $^{23}\text{Na}^{16}\text{O}^-$ in fully aged SSA. These results are completely consistent with the TEM and STEM observations in Figures 2, 4, and 8. Based on the mappings of $^{32}\text{S}^-$ (sulfate), $^{14}\text{N}^{16}\text{O}_2^-$ (nitrate), and $^{23}\text{Na}^{16}\text{O}^-$ in Figure 9, the nanoSIMS analysis provide direct evidence of Na_2SO_4 and NaNO_3 formation in fully aged SSA. As a result, sulfate and nitrate accumulated in SSA through atmospheric chemical reactions (e.g., reactions (R1)-(R4)) in the arctic area, which has been observed in polluted air by Laskin et al.(2012). These mapping results from STEM and nanoSIMS are consistent with the TEM/EDX results shown in Figs. 2-4 and with investigators who found that individual SSA in the Arctic air contained certain amounts of sulfate or nitrate by SEM/EDX and aerosol time-of-flight mass spectrometry (ATOFMS) (Hara et al., 2003;Geng et al., 2010;Sierau et al., 2014). However, we found that individual aged particles simultaneously contained sulfate and nitrate, suggesting individual SSA underwent heterogeneous reactions with different acidic gases during ageing processes in the arctic atmosphere. A number of studies found that a large fraction of SSA internally mixed with sulfate and nitrate occurred from coastal to background marine air and from equatorial to high latitudes (Andreae et al., 1986;Pósfai et al., 1994;Middlebrook et al., 1998;Hara et al., 2003;Geng et al., 2010;Li et al., 2011b;Yao and Zhang, 2011;Laskin et al., 2012). Interestingly, we noticed that fully aged SSA (Fig. 8C) had an elevated carbon content, suggesting that organic matter might occur in the aged SSA (the details in section 4.2). Laskin et al. (2012) showed that SSA can react with secondary organic acids and result in formation of organic salts in the polluted air.

Na mappings show that Na is absent in the coating of fresh SSA (Fig. 8A) but is present in minor amounts in the coating of partially aged SSA (Fig. 8B), which is consistent with the EDX results as shown in Figs. 2-3. In contrast, Mg, S, and O are absent from the core of fresh SSA (Fig. 8A) but are present in certain amounts within the core of partially aged SSA (Fig. 8B). Therefore, we can deduce that MgCl_2 coatings of the fresh SSA firstly reacted with acidic gases through chemical reactions (R1) and (R2) as the fresh SSA were transformed into the partially aged SSA. The

1 presence of MgCl_2 coatings in the fresh SSA is particularly interesting because it is
2 known to readily deliquesce at a considerably lower point (33% RH at 298 K) than
3 that of NaCl (75%) (Wise et al., 2009). We conclude, therefore, that this MgCl_2
4 coating consistently allowed an aqueous layer to coat the fresh SSA in the Arctic
5 atmosphere, because the ambient RH (56~94%) exceeded the deliquescence point.
6 Despite the relatively low concentration of MgCl_2 in SSA, the liquid surface
7 significantly enhances heterogeneous reactions rates through the uptake of acidic
8 gases (e.g., $\text{H}_2\text{SO}_4/\text{SO}_2$, and HNO_3/NO_x) (Liu et al., 2007). Microscopic observations
9 suggest that MgCl_2 on fresh SSA likely initiated and promoted the heterogeneous
10 reactions between SSA and acidic gases. To our knowledge, this is the first
11 demonstration of the influence of minor MgCl_2 in individual SSA in field studies,
12 although this phenomenon has been reported in laboratory experiments (Zhao et al.,
13 2006;Liu et al., 2007;Wise et al., 2009). In addition, MgCl_2 appears to have greater
14 importance in individual Arctic SSA than elsewhere because the $\text{Mg}^{2+}/\text{Na}^+$ ratio in
15 SSA increases following a temperature decrease (Hara et al., 2012). In the partially
16 aged particles, the new coating containing MgSO_4 , $\text{Mg}(\text{NO}_3)_2$, and NaNO_3 (Fig. 3)
17 likely remained as a supersaturated liquid coating on the surface of the ambient SSA
18 in the arctic area (Zhao et al., 2006;Li et al., 2008;Woods et al., 2010). Therefore, the
19 Mg-salts in fresh and partially aged SSA are important surfactants to speed up
20 particles ageing in the arctic area.

21 In this study we found an abundance of fully aged SSA in this arctic area (Figs.
22 4-6). Ault et al. (2013a) found that the Na^+ , Mg^{2+} and Ca^{2+} in individual SSA undergo
23 a spatial redistribution after heterogeneous reaction with nitric acid in the laboratory.
24 We noticed a similar phenomenon in which Na, Mg, and Ca mappings in particle C
25 were different from particles A and B (Fig. 8). Na is enhanced at the surface; Mg and
26 Ca tend to concentrate in the individual particle center. Figure 8C shows that carbon
27 intensity becomes strong in fully aged SSA, similar to the C-rich coating in Figs. 4c-d.
28 These results suggest that the aged SSA probably contain organic matter (the details in
29 section 4.2). In addition, most of the fully aged SSA have a Na_2SO_4 core coated with
30 NaNO_3 (with minor $\text{Mg}(\text{NO}_3)_2$ and MgSO_4) (Fig. 4). Hygroscopic experiments of

individual SSA exhibit that the surfaces of partially and fully aged SSA have earlier deliquescence than that of fresh SSA based on their hygroscopic growth on the substrate. The results indicate that the nitrate coatings likely influence particle surface deliquescence (Fig. S4). In the laboratory, the pure NaNO_3 can take up water starting at 25% RH and grow continuously with increasing RH (Lee and Hsu, 2000). Hu et al. (2010) also illustrated that NaNO_3 did not exhibit obvious deliquescence phenomenon in the hygroscopic experiment. As a result, some partially and fully aged Arctic SSA had liquid surfaces in ambient air (56~94% RH) and that this liquid amounted to certain amounts of water in these aerosol particles. Park et al. (2014) supplied the evidence of water in arctic particles through the hygroscopicity and volatility tandem differential mobility analyzer. The hygroscopic growth of particles can cause 1.6 to 3.7 times more negative aerosol direct radiative effects (Sand et al., 2013) than particles without it.

4.2 Organic matter in aged SSA

Integrated observations of individual SSA through the TEM, STEM, and nanoSIMS provided direct evidence of the occurrence of sulfate and nitrate in aged SSA in the arctic atmosphere. Laskin et al. (2012) showed that SSA effectively reacted with organic acids in polluted coastal air, leaving behind particles depleted in chloride and enriched in the corresponding organic salts. Moreover, substitution of Cl in SSA by weak organic acids was suggested in the laboratory by Ma et al. (2013). However, whether weak organic acids participated in the chloride depletion remains uncertain in the clean arctic air.

NanoSIMS technology has been adopted to characterize organic matter in SSA through $^{12}\text{C}^-$ and $^{12}\text{C}^{14}\text{N}^-$ mappings (Fig. 9). $^{12}\text{C}^-$ mapping of fresh SSA indicates extremely small amounts of organic matter in its coating (Fig. 9a). Tervahattu et al. (2002) found that organic films on SSA are common in fresh marine aerosols because of bursting bubbles from the spray of the waves. Quinn et al. (2015) also found that fresh SSA are internally mixed with organic matter in the northeastern Atlantic atmosphere using proton nuclear magnetic resonance (^1H NMR). In comparison with fresh SSA in Figure 9a, the $^{12}\text{C}^-$ intensity of the aged SSA in Figure 9b was much

enhanced. The only explanation is that more organic matter from the atmosphere was incorporated into the aged SSA. Similar phenomena in aged SSA have been observed by laser mass spectrometry at Cape Grim and the amounts of additional sulfate and organic matter in individual particles may be an indication of particles ageing (Middlebrook et al., 1998). Additionally, with increasing organic matter in SSA, their morphology and crystallization behavior changes (Ault et al., 2013b).

Interestingly, $^{12}\text{C}^-$ line scan in aged SSA further indicates that organic matter is mostly restricted to their surfaces (Fig. 9b). The near edge X-ray absorption fine structure spectroscopy (NEXAFS) carbon K-edge spectrum of the organic phase reveals a dominant contribution from carboxylic acids on the surface of the aged SSA (Laskin et al., 2012). We further found organic matter internally mixed with nitrate on the surface for aged SSA. This finding supports the results from laboratory experiments and conforms to predictions of liquid-liquid phase separation theory (Ault et al., 2013a). As a result, we obtained one conceptual model based on these above findings summarizing the possible SSA ageing processes in the arctic atmosphere (Fig. 10).

The nanoSIMS analyses of the aged SSA in the arctic air show that their surface layers commonly contain organic matter. The organic layer may influence trace gas uptake, and subsequently impact trace gas budgets of O_3 and NO_2 in the arctic (McNeill et al., 2006). This is the first demonstration of organic-coated SSA in clean arctic air, which extends the application of heterogeneous reactions on aerosol particles (Fig. 10). Comparisons of fresh and aged SSA in Fig. 9 suggest that these organic coatings likely took part in the chloride depletion during particles ageing. The chloride depletion in the SSA induced by the presence of organic acids should be incorporated into the atmospheric chemistry models for clean marine air, in addition to the coastal urban regions reported by Laskin et al. (2012). Randles et al. (2014) reported that NaCl internally mixed with organic matter can reduce radiative cooling substantially compared to pure NaCl aerosol in the laboratory. In addition, how the organic layer influences hygroscopic and optical properties of the aged SSA in realistic atmospheres remains unknown. Our measurements make clear the need to

1 understand SSA's complexity in arctic air.

2 In summary, our results indicate that formation of sulfate, nitrate, and organic
3 salts in the SSA can remove trace gases (e.g., organic acids, $\text{H}_2\text{SO}_4/\text{SO}_2$, and
4 HNO_3/NO_x) in the arctic air, which were mostly emitted by various anthropogenic
5 sources from middle latitudes (Law and Stohl, 2007; Chang et al., 2011). On the one
6 hand, the results of these heterogeneous reactions could change the CCN or IN
7 abilities, optical properties, and further dry and wet deposition of SSA. On the other
8 hand, these surface reactions of SSA could affect the photochemical reactivity in the
9 Arctic air because they release gaseous halogen species (De Haan et al.,
10 1999; Knipping et al., 2000; von Glasow, 2008; Thornton et al., 2010).

11 **5 Conclusions**

12 TEM observations indicated that SSA were most abundant from 100 nm to 10
13 μm in the summer arctic atmosphere, accounting for about 72% of the total aerosol
14 particles. Three types of SSA, fresh SSA, partially aged SSA, and fully aged SSA,
15 were identified based on their morphology and composition. The fresh SSA particles
16 exhibited a single core-shell structure. Containing only Na and Cl, the core consisted
17 of the cubic NaCl crystal with the coating of Mg, Ca, S, O and Cl, identified as CaSO_4
18 and MgCl_2 . Individual partially aged SSA particles consisted of the single irregularly
19 shaped NaCl core coated with Na, Mg, Ca, K, N, O, and S, with or without minor Cl,
20 suggesting a single Cl-depletion phenomenon in the formation of partially aged SSA.
21 The fully aged SSA lack the NaCl core, suggesting that the Cl in SSA was completely
22 depleted through heterogeneous chemical reactions. Nonetheless, most fully aged SSA
23 consist of the Na_2SO_4 core with the amorphous NaNO_3 coating.

24 STEM further determined the elemental mappings of Na, Mg, Ca, Cl, S, O, C,
25 and N in the three kinds of SSA. We found that Cl content decreases and S, O, C and
26 N contents increase along with particles ageing from partially to fully aged SSA.
27 NanoSIMS technology has been employed to obtain secondary ion intensity mappings
28 of $^{12}\text{C}^-$, $^{16}\text{O}^-$, $^{12}\text{C}^{14}\text{N}^-$, $^{14}\text{N}^{16}\text{O}_2^-$, $^{32}\text{S}^-$, $^{35}\text{Cl}^-$, and $^{23}\text{Na}^{16}\text{O}^-$. $^{14}\text{N}^{16}\text{O}_2^-$ and $^{23}\text{Na}^{16}\text{O}^-$
29 mappings proved NaNO_3 formation in fully aged SSA. These results show that sulfate
30 and nitrate formed in SSA through atmospheric chemical reactions in arctic area. In

1 addition, MgCl_2 coating on fresh SSA can induce heterogeneous reactions between
2 SSA and acidic gases because MgCl_2 is known to readily deliquesce at a considerably
3 lower point (33% RH at 298 K) than that of NaCl (75%). The partially and fully aged
4 SSA were expected to have liquid surfaces (MgSO_4 , MgNO_3 , and NaNO_3) in arctic
5 ambient air (56~94% RH); such surfaces contain substantial amounts of water, so the
6 coating contents were conducive to accelerate the heterogeneous reactions. ^{12}C -
7 mapping of individual fresh SSA obtained by nanoSIMS indicate extremely small
8 amounts of organic matter in the coating of the particle, although this organic matter
9 was somewhat enhanced in the aged SSA. We also found that organic matter was
10 mostly limited to the particle surface.

11 The composition of the SSA and their internal heterogeneity likely have
12 important effects on their hygroscopic and optical properties, dynamics of phase
13 separations, and heterogeneous reaction with inorganic and organic acidic gases.
14 These microscopic observations for SSA provide insights into the system of
15 gas-aerosol-climate in the arctic atmosphere.

16

17 **Acknowledgements**

18 We appreciate Peter Hyde's comments and proofreading. This work was funded
19 by National Natural Science Foundation of China (41575116), Shandong Natural
20 Science Funds for Distinguished Young Scholar (JQ201413), Young Scholars
21 Program of Shandong University (2015WLJH37), China Polar Science Strategy
22 Research Foundation (20140310), and Fundamental Research Funds of Shandong
23 University (2014QY001). We gratefully acknowledge the NOAA Air Resources
24 Laboratory (ARL) for the provision of the HYSPLIT transport used in this
25 publication.

References

- Allen, H. C., Laux, J. M., Vogt, R., Finlayson-Pitts, B. J., and Hemminger, J. C.: Water-induced reorganization of ultrathin nitrate films on NaCl: implications for the tropospheric chemistry of sea salt particles, *J. Phys. Chem.*, 100, 6371-6375, doi:10.1021/jp953675a, 1996.
- Andreae, M. O., Charlson, R. J., Bruynseels, F., Storms, H., Van Grieken, R., and Maeahaut, W.: Internal mixture of sea salt, silicates, and excess sulfate in marine aerosols, *Science*, 232, 1620-1623, doi:10.1126/science.232.4758.1620, 1986.
- Ault, A. P., Peters, T. M., Sawvel, E. J., Casuccio, G. S., Willis, R. D., Norris, G. A., and Grassian, V. H.: Single-particle SEM-EDX analysis of iron-containing coarse particulate matter in an urban environment: sources and distribution of iron within Cleveland, Ohio, *Environ. Sci. Technol.*, 46, 4331-4339, 2012.
- Ault, A. P., Guasco, T. L., Ryder, O. S., Baltrusaitis, J., Cuadra-Rodriguez, L. A., Collins, D. B., Ruppel, M. J., Bertram, T. H., Prather, K. A., and Grassian, V. H.: Inside versus outside: ion redistribution in nitric acid reacted sea spray aerosol particles as determined by single particle analysis, *J. Am. Chem. Soc.*, 135, 14528-14531, doi:10.1021/ja407117x, 2013a.
- Ault, A. P., Moffet, R. C., Baltrusaitis, J., Collins, D. B., Ruppel, M. J., Cuadra-Rodriguez, L. A., Zhao, D., Guasco, T. L., Ebben, C. J., Geiger, F. M., Bertram, T. H., Prather, K. A., and Grassian, V. H.: Size-dependent changes in sea spray aerosol composition and properties with different seawater conditions, *Environ. Sci. Technol.*, 47, 5603-5612, doi:10.1021/es400416g, 2013b.
- Barrie, L. A.: Arctic air pollution: an overview of current knowledge, *Atmos. Environ.*, 20, 643-663, 1986.
- Chang, R. Y. W., Leck, C., Graus, M., Müller, M., Paatero, J., Burkhardt, J. F., Stohl, A., Orr, L. H., Hayden, K., Li, S. M., Hansel, A., Tjernström, M., Leaitch, W. R., and Abbatt, J. P. D.: Aerosol composition and sources in the central Arctic Ocean during ASCOS, *Atmos. Chem. Phys.*, 11, 10619-10636, doi:10.5194/acp-11-10619-2011, 2011.
- Conny, J. M., and Norris, G. A.: Scanning electron microanalysis and analytical

1 challenges of mapping elements in urban atmospheric particles, *Environ. Sci. Technol.*,
2 45, 7380-7386, 2011.

3 De Haan, D. O., Brauers, T., Oum, K., Stutz, J., Nordmeyer, T., and Finlayson-Pitts, B.
4 J.: Heterogeneous chemistry in the troposphere: experimental approaches and
5 applications to the chemistry of sea salt particles, *Int. Rev. Phys. Chem.*, 18, 343-385,
6 1999.

7 Gard, E. E., Kleeman, M. J., Gross, D. S., Hughes, L. S., Allen, J. O., Morrical, B. D.,
8 Fergenson, D. P., Dienes, T., Gälli, M. E., and Johnson, R. J.: Direct observation of
9 heterogeneous chemistry in the atmosphere, *Science*, 279, 1184-1187, 1998.

10 Geng, H., Ryu, J., Jung, H.-J., Chung, H., Ahn, K.-H., and Ro, C.-U.: Single-particle
11 characterization of summertime arctic aerosols collected at Ny-Alesund, Svalbard,
12 *Environ. Sci. Technol.*, 44, 2348-2353, doi:10.1021/es903268j, 2010.

13 Ghorai, S., Wang, B., Tivanski, A., and Laskin, A.: Hygroscopic properties of
14 internally mixed particles composed of NaCl and water-soluble organic acids, *Environ.*
15 *Sci. Technol.*, 48, 2234-2241, doi:10.1021/es404727u, 2014.

16 Goto-Azuma, K., and Koerner, R. M.: Ice core studies of anthropogenic sulfate and
17 nitrate trends in the Arctic, *J. Geophys. Res.-Atmos.*, 106, 4959-4969,
18 doi:10.1029/2000jd900635, 2001.

19 Hara, K., Yamagata, S., Yamanouchi, T., Sato, K., Herber, A., Iwasaka, Y., Nagatani,
20 M., and Nakata, H.: Mixing states of individual aerosol particles in spring Arctic
21 troposphere during ASTAR 2000 campaign, *J. Geophys. Res.-Atmos.*, 108, 4209,
22 doi:10.1029/2002jd002513, 2003.

23 Hara, K., Osada, K., Yabuki, M., and Yamanouchi, T.: Seasonal variation of
24 fractionated sea-salt particles on the Antarctic coast, *Geophys. Res. Lett.*, 39, L18801,
25 doi:10.1029/2012gl052761, 2012.

26 Hegg, D. A., Warren, S. G., Grenfell, T. C., Doherty, S. J., Larson, T. V., and Clarke, A.
27 D.: Source attribution of black carbon in Arctic snow, *Environ. Sci. Technol.*, 43,
28 4016-4021, doi:10.1021/es803623f, 2009.

29 Heintzenberg: Particle size distribution and optical properties of Arctic haze, *Tellus*,
30 32, 251-260, 1980.

1 Hu, D., Qiao, L., Chen, J., Ye, X., Yang, X., Cheng, T., and Fang, W.: Hygroscopicity
2 of inorganic aerosols: size and relative humidity effects on the growth factor, *Aerosol*
3 *Air Qual. Res.*, 10, 255-264, 2010.

4 Hu, R. M., Blanchet, J. P., and Girard, E.: Evaluation of the direct and indirect
5 radiative and climate effects of aerosols over the western Arctic, *J. Geophys.*
6 *Res.-Atmos.*, 110, D11213, doi:10.1029/2004jd005043, 2005.

7 Iziomon, M. G., Lohmann, U., and Quinn, P. K.: Summertime pollution events in the
8 Arctic and potential implications, *J. Geophys. Res.-Atmos.*, 111, D12206,
9 doi:10.1029/2005jd006223, 2006.

10 Knipping, E. M., Lakin, M. J., Foster, K. L., Jungwirth, P., Tobias, D. J., Gerber, R. B.,
11 Dabdub, D., and Finlayson-Pitts, B. J.: Experiments and simulations of ion-enhanced
12 interfacial chemistry on aqueous NaCl aerosols, *Science*, 288, 301-306,
13 doi:10.1126/science.288.5464.301, 2000.

14 Kouyoumdjian, H., and Saliba, N.: Mass concentration and ion composition of coarse
15 and fine particles in an urban area in Beirut: effect of calcium carbonate on the
16 absorption of nitric and sulfuric acids and the depletion of chloride, *Atmos. Chem.*
17 *Phys.*, 6, 1865-1877, doi:10.5194-acp-6-1865-2006, 2006.

18 Laskin, A., Moffet, R. C., Gilles, M. K., Fast, J. D., Zaveri, R. A., Wang, B., Nigge, P.,
19 and Shutthanandan, J.: Tropospheric chemistry of internally mixed sea salt and
20 organic particles: surprising reactivity of NaCl with weak organic acids, *J. Geophys.*
21 *Res.-Atmos.*, 117, D15302, doi:10.1029/2012jd017743, 2012.

22 Law, K. S., and Stohl, A.: Arctic air pollution: origins and impacts, *Science*, 315,
23 1537-1540, doi:10.1126/science.1137695, 2007.

24 Leck, C., and Svensson, E.: Importance of aerosol composition and mixing state for
25 cloud droplet activation over the Arctic pack ice in summer, *Atmos. Chem. Phys.*, 15,
26 2545-2568, doi:10.5194/acp-15-2545-2015, 2015.

27 Lee, C.-T., and Hsu, W.-C.: The measurement of liquid water mass associated with
28 collected hygroscopic particles, *J. Aerosol Sci.*, 31, 189-197, 2000.

29 Li, W., Li, P., Sun, G., Zhou, S., Yuan, Q., and Wang, W.: Cloud residues and
30 interstitial aerosols from non-precipitating clouds over an industrial and urban area in

1 northern China, *Atmos. Environ.*, 45, 2488-2495, 2011a.

2 Li, W., Shao, L., Shen, R., Yang, S., Wang, Z., and Tang, U.: Internally mixed sea salt,
3 soot, and sulfates at Macao, a coastal city in South China, *J. Air Waste Manage.*, 61,
4 1166-1173, doi:10.1080/10473289.2011.603996, 2011b.

5 Li, W., Wang, T., Zhou, S., Lee, S., Huang, Y., Gao, Y., and Wang, W.: Microscopic
6 observation of metal-containing particles from Chinese continental outflow observed
7 from a non-industrial site, *Environ. Sci. Technol.*, 47, 9124-9131,
8 doi:10.1021/es400109q, 2013a.

9 Li, W., Wang, Y., Collett, J. L., Chen, J., Zhang, X., Wang, Z., and Wang, W.:
10 Microscopic evaluation of trace metals in cloud droplets in an acid precipitation
11 region, *Environ. Sci. Technol.*, 47, 4172-4180, doi:10.1021/es304779t, 2013b.

12 Li, W. J., and Shao, L. Y.: Transmission electron microscopy study of aerosol particles
13 from the brown hazes in Northern China, *J. Geophys. Res.-Atmos.*, 114, D09302,
14 doi:10.1029/2008JD011285, 2009.

15 Li, X. H., Zhao, L. J., Dong, J. L., Xiao, H. S., and Zhang, Y. H.: Confocal Raman
16 studies of $\text{Mg}(\text{NO}_3)_2$ aerosol particles deposited on a quartz substrate: supersaturated
17 structures and complicated phase transitions, *J. Phys. Chem. B*, 112, 5032-5038,
18 doi:10.1021/jp709938x, 2008.

19 Lindsay, R., Zhang, J., Schweiger, A., Steele, M., and Stern, H.: Arctic sea ice retreat
20 in 2007 follows thinning trend, *J. Climate*, 22, 165-176, 2009.

21 Liu, Y., Cain, J. P., Wang, H., and Laskin, A.: Kinetic study of heterogeneous reaction
22 of deliquesced NaCl particles with gaseous HNO_3 using particle-on-substrate
23 stagnation flow reactor approach, *J. Phys. Chem. A*, 111, 10026-10043,
24 doi:10.1021/jp072005p, 2007.

25 Ma, Q., Ma, J., Liu, C., Lai, C., and He, H.: Laboratory Study on the Hygroscopic
26 Behavior of External and Internal C2–C4 Dicarboxylic Acid–NaCl Mixtures, *Environ.*
27 *Sci. Technol.*, 47, 10381-10388, doi:10.1021/es4023267, 2013.

28 McNeill, V. F., Patterson, J., Wolfe, G. M., and Thornton, J. A.: The effect of varying
29 levels of surfactant on the reactive uptake of N_2O_5 to aqueous aerosol, *Atmos. Chem.*
30 *Phys.*, 6, 1635-1644, doi:10.5194/acp-6-1635-2006, 2006.

1 Middlebrook, A. M., Murphy, D. M., and Thomson, D. S.: Observations of organic
2 material in individual marine particles at Cape Grim during the first aerosol
3 characterization experiment (ACE 1), *J. Geophys. Res.-Atmos.*, 103, 16475-16483,
4 doi:10.1029/97jd03719, 1998.

5 Murphy, D. M., Anderson, J. R., Quinn, P. K., McInnes, L. M., Brechtel, F. J.,
6 Kreidenweis, S. M., Middlebrook, A. M., Posfai, M., Thomson, D. S., and Buseck, P.
7 R.: Influence of sea-salt on aerosol radiative properties in the Southern Ocean marine
8 boundary layer, *Nature*, 392, 62-65, 1998.

9 O'Dowd, C. D., Smith, M. H., Consterdine, I. E., and Lowe, J. A.: Marine aerosol,
10 sea-salt, and the marine sulphur cycle: a short review, *Atmos. Environ.*, 31, 73-80,
11 1997.

12 O'Dowd, C. D., and De Leeuw, G.: Marine aerosol production: a review of the current
13 knowledge, *Philos. T. R. Soc. A*, 365, 1753-1774, 2007.

14 Pósfai, M., Anderson, J. R., Buseck, P. R., Shattuck, T. W., and Tindale, N. W.:
15 Constituents of a remote pacific marine aerosol: a TEM study, *Atmos. Environ.*, 28,
16 1747-1756, 1994.

17 Park, K., Kim, G., Kim, J.-s., Yoon, Y.-J., Cho, H.-j., and Ström, J.: Mixing state of
18 size-selected submicrometer particles in the Arctic in May and September 2012,
19 *Environ. Sci. Technol.*, 48, 909-919, doi:10.1021/es404622n, 2014.

20 Quinn, P. K., Collins, D. B., Grassian, V. H., Prather, K. A., and Bates, T. S.:
21 Chemistry and related properties of freshly emitted sea spray aerosol, *Chem. Rev.*,
22 doi:10.1021/cr500713g, 2015.

23 Rastak, N., Silvergren, S., Zieger, P., Wideqvist, U., Ström, J., Svenningsson, B.,
24 Maturilli, M., Tesche, M., Ekman, A. M., and Tunved, P.: Seasonal variation of
25 aerosol water uptake and its impact on the direct radiative effect at Ny-Ålesund,
26 Svalbard, *Atmos. Chem. Phys.*, 14, 7445-7460, 2014.

27 Rossi, M. J.: Heterogeneous reactions on salts, *Chem. Rev.*, 103, 4823-4882, 2003.

28 Sand, M., Berntsen, T. K., Kay, J. E., Lamarque, J. F., Seland, Ø., and Kirkevåg, A.:
29 The Arctic response to remote and local forcing of black carbon, *Atmos. Chem. Phys.*,
30 13, 211-224, doi:10.5194/acp-13-211-2013, 2013.

1 Serreze, M. C., and Francis, J. A.: The Arctic amplification debate, *Climatic Change*,
2 76, 241-264, 2006.

3 Shaw, G. E.: The Arctic haze phenomenon, *B. Am. Meteorol. Soc.*, 76, 2403-2413,
4 1995.

5 Sierau, B., Chang, R. Y. W., Leck, C., Paatero, J., and Lohmann, U.: Single-particle
6 characterization of the high-Arctic summertime aerosol, *Atmos. Chem. Phys.*, 14,
7 7409-7430, doi:10.5194/acp-14-7409-2014, 2014.

8 Tervahattu, H., Hartonen, K., Kerminen, V. M., Kupiainen, K., Aarnio, P., Koskentalo,
9 T., Tuck, A. F., and Vaida, V.: New evidence of an organic layer on marine aerosols, *J.*
10 *Geophys. Res.-Atmos.*, 107, 4053, doi:10.1029/2000jd000282, 2002.

11 Thornton, J. A., Kercher, J. P., Riedel, T. P., Wagner, N. L., Cozic, J., Holloway, J. S.,
12 Dubé W. P., Wolfe, G. M., Quinn, P. K., Middlebrook, A. M., Alexander, B., and
13 Brown, S. S.: A large atomic chlorine source inferred from mid-continental reactive
14 nitrogen chemistry, *Nature*, 464, 271-274, 2010.

15 Vavrus, S.: The impact of cloud feedbacks on Arctic climate under greenhouse forcing,
16 *J. Climate*, 17, 603-615, 2004.

17 von Glasow, R.: Atmospheric chemistry: pollution meets sea salt, *Nature Geosci.*, 1,
18 292-293, 2008.

19 Wise, M. E., Freney, E. J., Tyree, C. A., Allen, J. O., Martin, S. T., Russell, L. M., and
20 Buseck, P. R.: Hygroscopic behavior and liquid-layer composition of aerosol particles
21 generated from natural and artificial seawater, *J. Geophys. Res.-Atmos.*, 114, 8,
22 doi:10.1029/2008jd010449, 2009.

23 Woods, E., Chung, D., Lanney, H. M., and Ashwell, B. A.: Surface morphology and
24 phase transitions in mixed NaCl/MgSO₄ aerosol particles, *J. Phys. Chem. A*, 114,
25 2837-2844, doi:10.1021/jp911133j, 2010.

26 Yao, X., and Zhang, L.: Chemical processes in sea-salt chloride depletion observed at
27 a Canadian rural coastal site, *Atmos. Environ.*, 46, 189-194,
28 doi:10.1016/j.atmosenv.2011.09.081, 2011.

29 Zhao, L. J., Zhang, Y. H., Wei, Z. F., Cheng, H., and Li, X. H.: Magnesium sulfate
30 aerosols studied by FTIR spectroscopy: hygroscopic properties, supersaturated

1 structures, and implications for seawater aerosols, J. Phys. Chem. A, 110, 951-958,
2 2006.
3

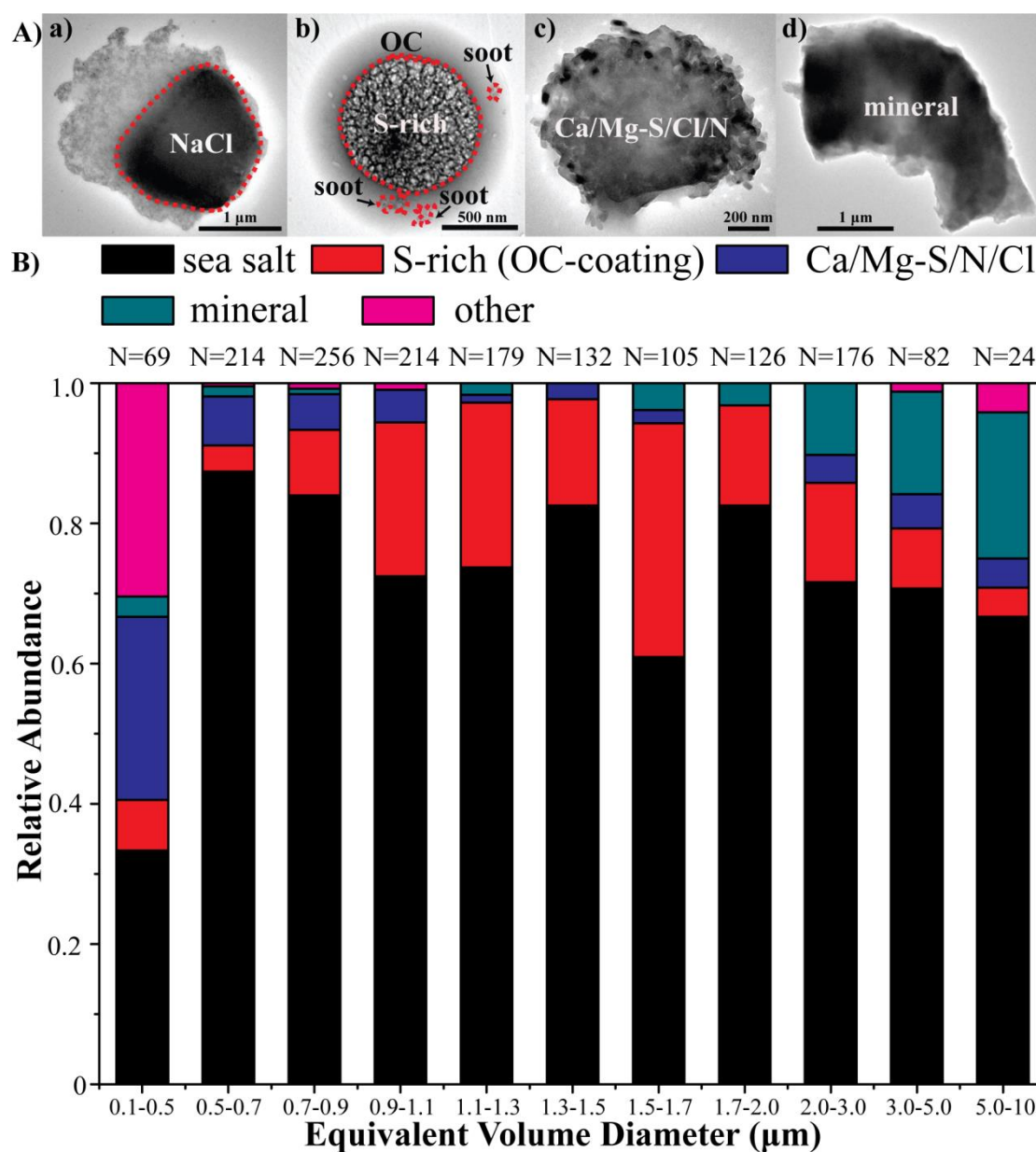


Figure 1. Morphology and relative abundances of typical individual aerosol particles in summertime Arctic samples: (A) TEM images of four types of aerosol particles, (B) relative abundances of different particle size ranges. The number of the analyzed particles in different size ranges is shown above each column.

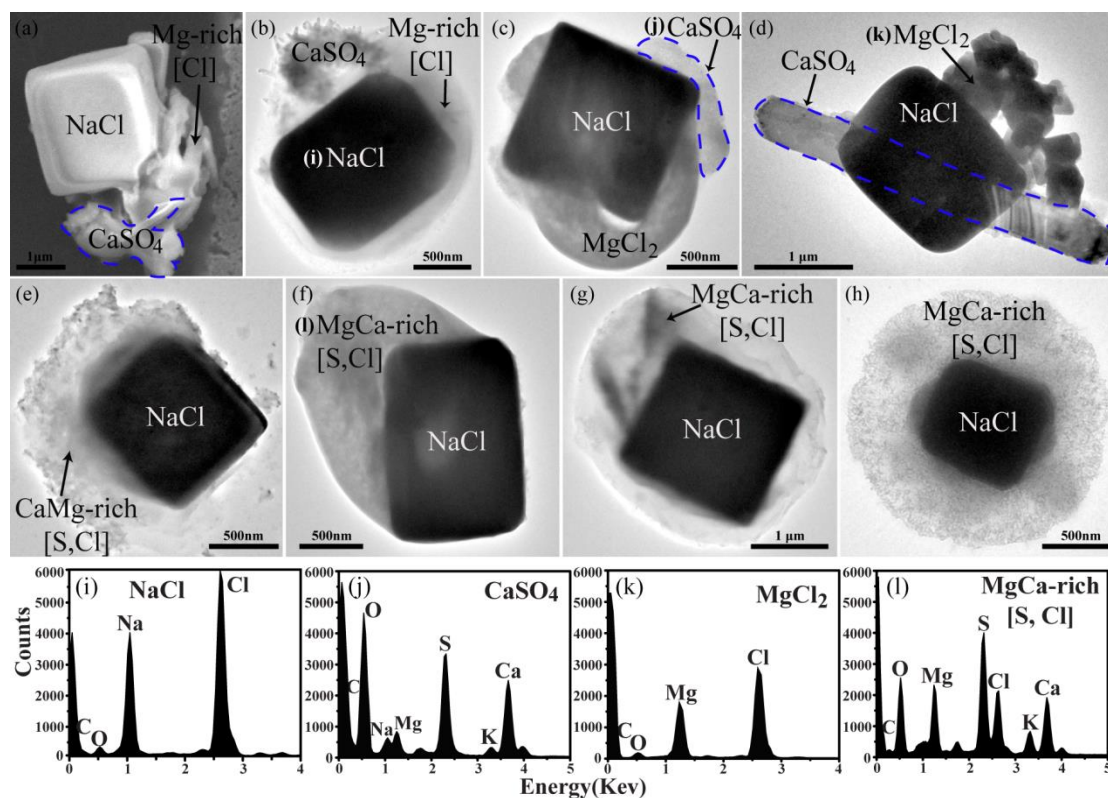


Figure 2. Morphology and EDX spectra of the typical fresh SSA. (a) One SEM image, (b)-(h) TEM images, and (i)-(h) EDX spectra of NaCl, MgCl₂, CaSO₄, and MgCa-rich. The main anionic elements are shown in the square brackets.

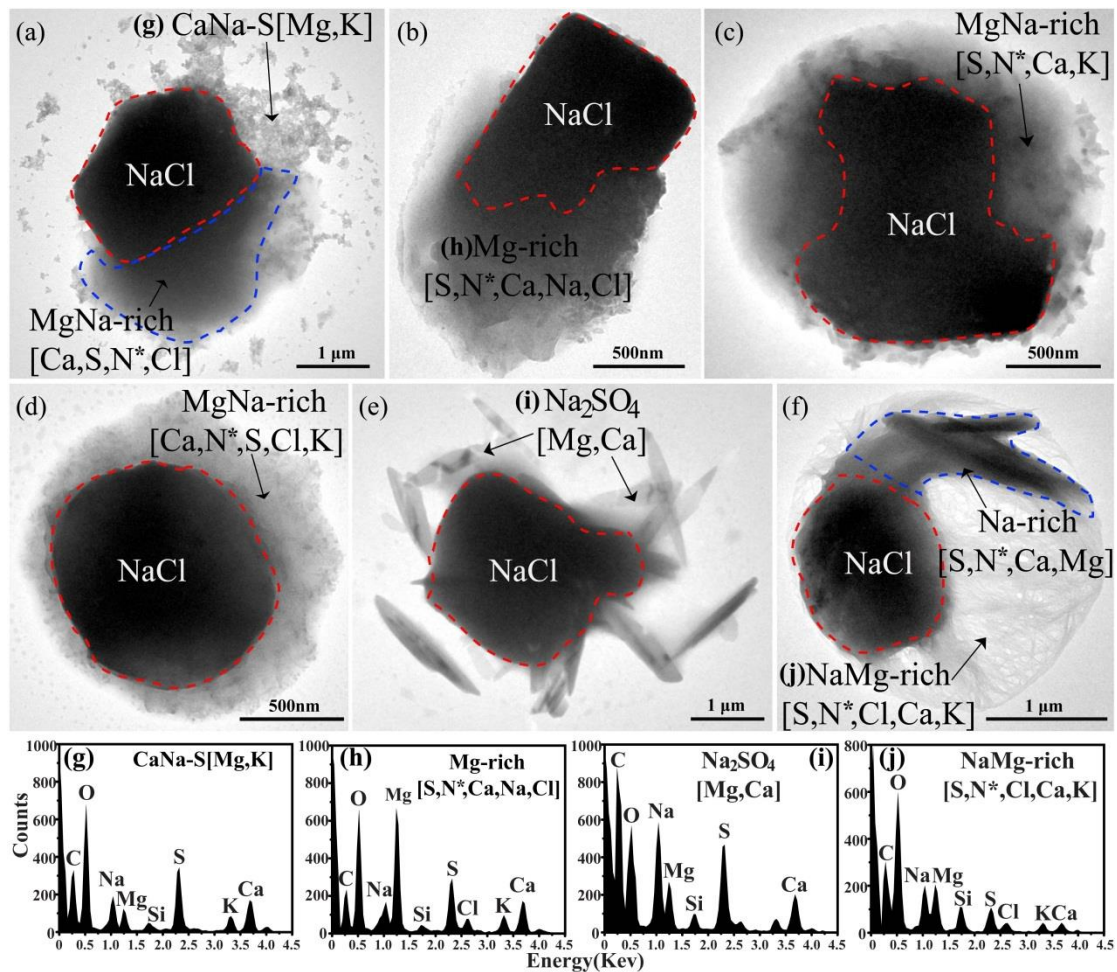


Figure 3. TEM images of typical partially aged SSA and EDX spectra of their coatings. (a-b) NaCl partially surrounded by the mixed species, containing Mg, Ca, Na, S, O, N and minor Cl; (c-d) NaCl completely surrounded by the mixed species with Mg, Ca, Na, S, O, N and minor Cl; (e-f) The rod-like Na₂SO₄ particles (minor Mg, and Ca) associated with NaCl. (g-j) The EDX spectra of one selected area in the internally mixed coating, including Na, Ca, Mg, S, and O with minor Cl and K. N cannot be directly measured but inferred based on elemental composition in aerosols.

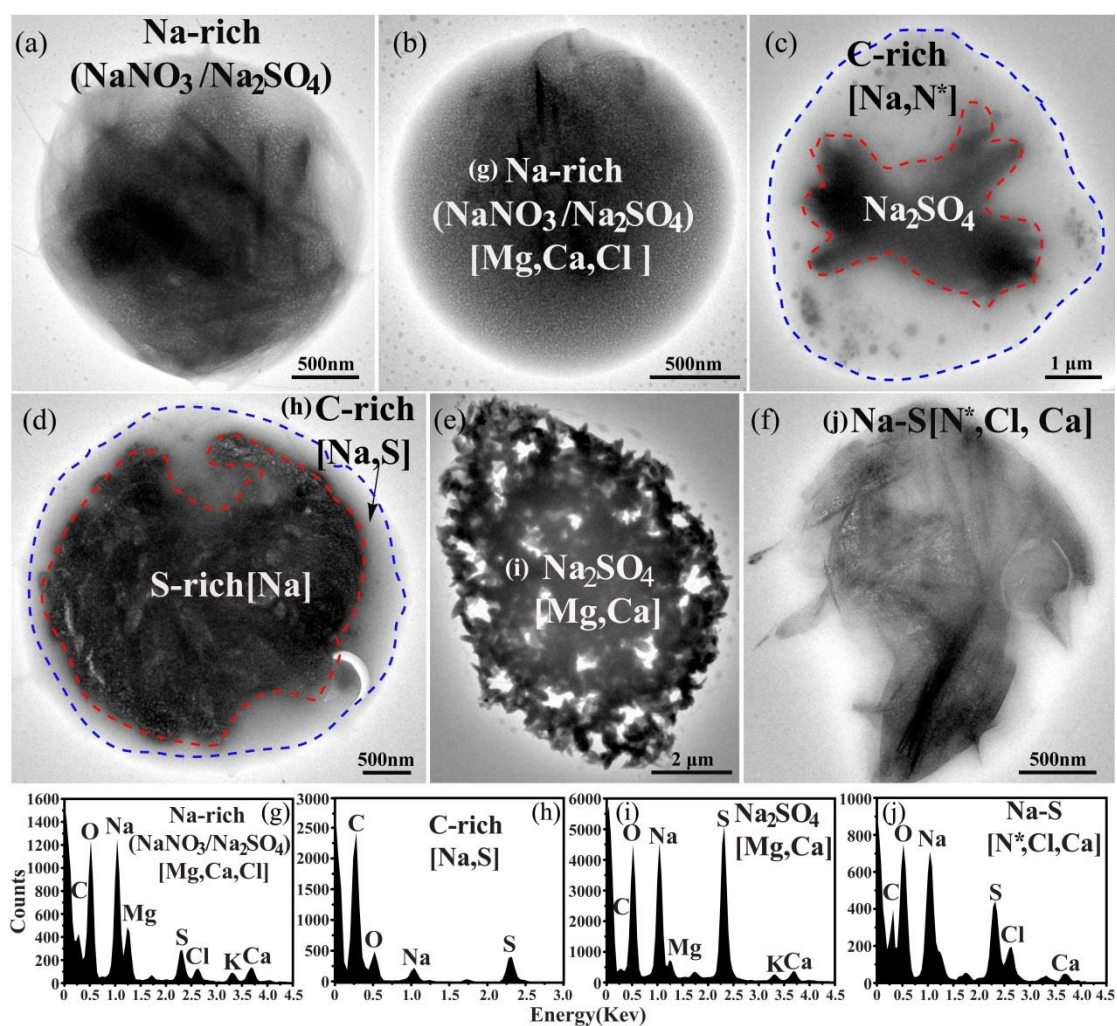


Figure 4. TEM images and EDX spectra of the typical fully aged SSA. Major species are shown in parentheses, and minor elements are in square brackets. (a-b) This Na-rich particle contains mostly Na, O, N, and S. The rod-like aggregates are Na_2SO_4 and the species of no-defined shape are NaNO_3 . The NaNO_3 -containing coating is more sensitive to the strong electron beam than the Na_2SO_4 . (c-d) Na-rich particles mainly contain C, N, O, Na, and S. One typical transparent coating with high C and minor O, Na, S or N, was stable under a strong electron beam, suggesting a possible organic coating. (e-f) The particles mainly contain Na, O, and S. Many small rod-like Na_2SO_4 gather together to form one particle. (g-j) EDX spectra of one selected part within individual SSA marked in TEM images. N cannot be directly measured but inferred based on elemental composition in aerosols.

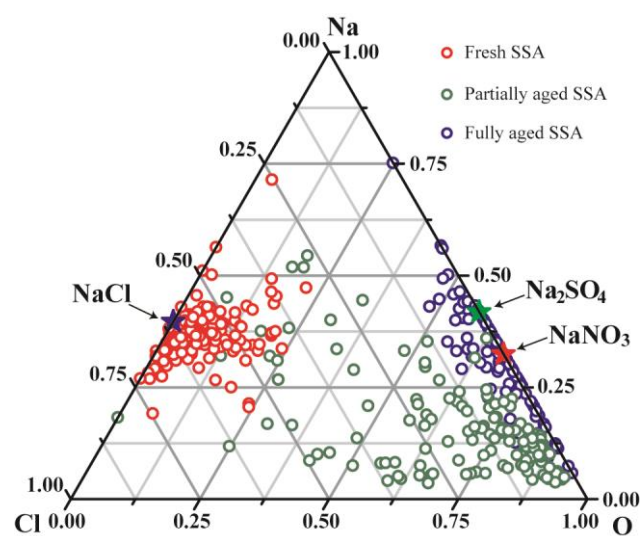


Figure 5. Triangular diagram of Na-Cl-O showing EDX data of elemental composition of 405 SSA. Three stars represent elemental composition of pure NaCl, Na_2SO_4 , and NaNO_3 , respectively.

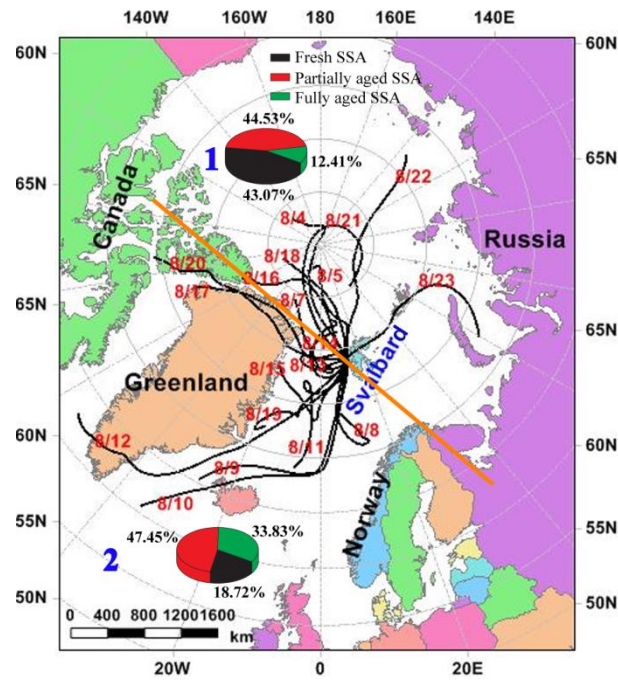


Figure 6. 72-h back trajectories of air masses at 500 m over Arctic Yellow River Station in Svalbard during 3-23 August, 2012, and arriving time was setting according to the sampling time. Air masses were divided into two groups by the yellow line: one group from central Arctic Ocean and other one from North America and Greenland. Pie charts showed the number fractions of the fresh, partially aged, and fully aged SSA.

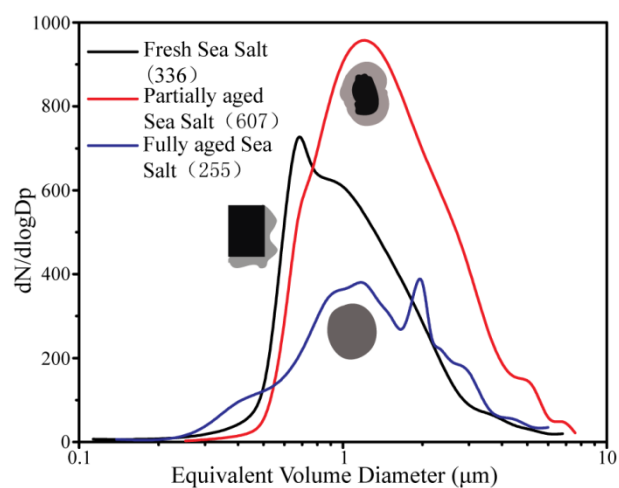


Figure 7. Size distributions of 336 fresh, 607 partially aged, and 255 fully aged SSA collected in Arctic summer. The SSA with diameters lower than 100 nm were not considered in this study.

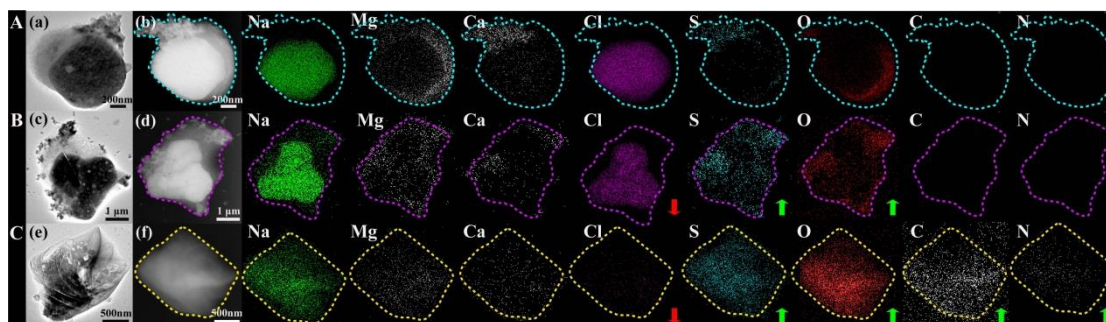


Figure 8. Bright and dark-field TEM images of the fresh, partially aged, and fully aged SSA and elemental mapping of Na, Mg, Ca, Cl, S, O, C, and N. (A) One fresh SSA particle, (B) One partially aged SSA particle, (C) One fully aged SSA particle. The dot intensity represents elemental concentration within an individual particle. The arrows in particles B and C represent increase or decrease of elemental concentration compared to the particle A.

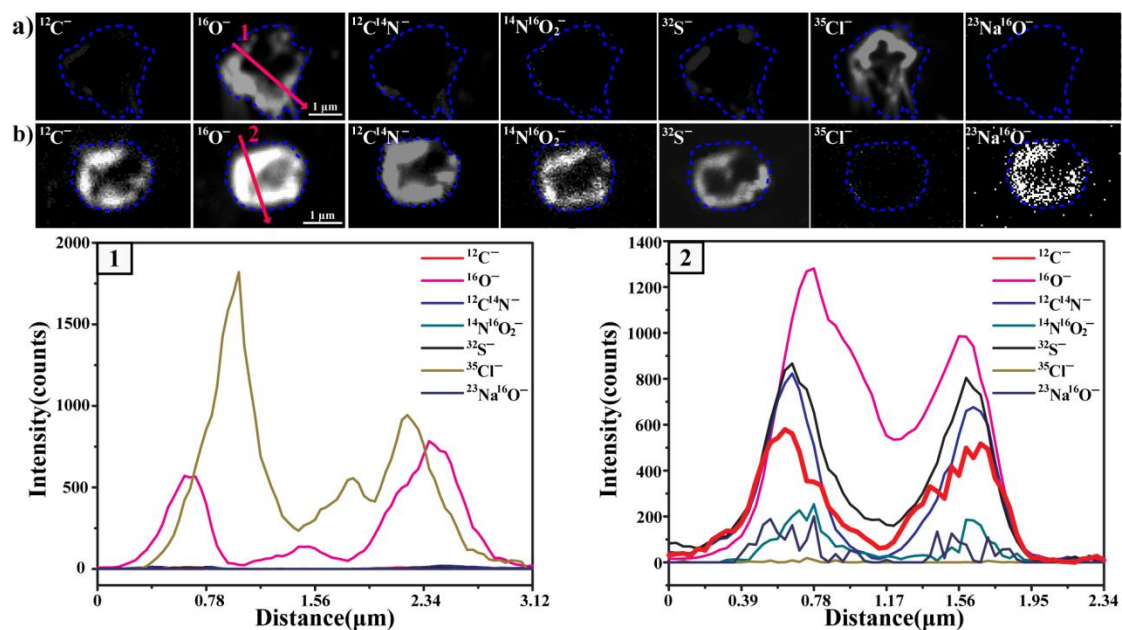


Figure 9. NanoSIMS-based ion intensity mappings. Mappings of $^{12}\text{C}^-$, $^{16}\text{O}^-$, $^{12}\text{C}^{14}\text{N}^-$, $^{14}\text{N}^{16}\text{O}_2^-$, $^{32}\text{S}^-$, $^{35}\text{Cl}^-$, and $^{23}\text{Na}^{16}\text{O}^-$ from one fresh SSA particle (a) and one fully aged SSA (b). Lines 1-2 represent the line scanning on the surfaces of individual particles. The red line represents the profile of $^{12}\text{C}^-$ in fully aged SSA.

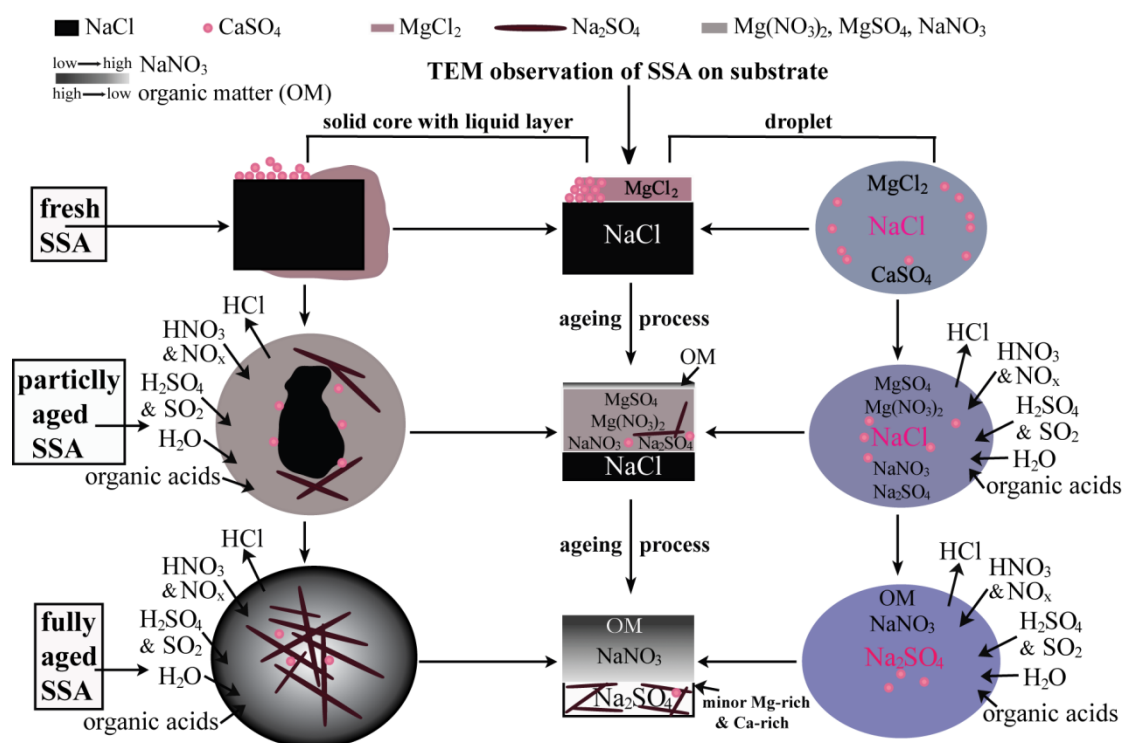


Figure 10. The conceptual model based on our study summarizing the possible SSA ageing processes from fresh, partially aged, and fully aged SSA. Deliquescence RH (DRH) of NaCl is at 75%. SSA ageing could have different processes before and after the DRH.